DOI: https://doi.org/10.15407/techned2026.01.032

TORQUE AND MAGNET HEATING IN A SURFACE-MOUNTED PM MOTOR: A COMPARISON BETWEEN SLOTTED AND SLOTLESS STATOR DESIGNS

I.S. Petukhov*, **Ye.V. Isaiev**
Institute of Electrodynamics National Academy of Sciences of Ukraine,
56, Beresteiskyi Ave., Kyiv, 03057, Ukraine.
E-mail: igor_petu@ukr.net.

The advantages and disadvantages of two permanent magnet motor designs – slotted and slotless – are analyzed. A commercially available micromotor was adopted as the slotted design. Their performance is compared in terms of torque production and permanent magnet heating under intensive operating conditions. The rotor geometry was assumed to be identical, the maximum flux density in the magnetic cores was set to 1,7 T, and the rotational speed was considered constant. Modeling was carried out using COMSOL Multiphysics, with the results for the slotted design validated using the Simcenter Motorsolve software package. The torque and the amplitude of torque pulsations for both designs were evaluated, and the differences between them were analyzed. The causes of magnetic flux density pulsations in the magnets were studied, and their impact on eddy current losses was assessed. Numerical results for the output parameter ratios of the two designs were presented. The possibility of neglecting magnet heating in the slotless design was emphasized. References 11, figures 8, table 1.
Ключові слова: PM motor, torque, eddy current losses, slotted design, slotless design.

Introduction. Permanent magnet (PM) motors have found widespread use in many technological applications due to their high specific power and torque compared to induction and DC machines. The best performance is usually achieved with conventional slotted stator designs. However, in the field of micromachine development, there is a growing interest in slotless designs [1–4]. Despite being generally inferior to slotted motors in terms of specific power, torque, and weight [5], slotless motors offer key advantages: simpler construction, lower manufacturing cost, and the absence of cogging torque. These features make them especially suitable for controlled precision drives, where low torque ripple is critical. Thus, when cost or torque smoothness is prioritized, the slotless configuration may be preferred, even though it typically results in reduced torque output.

An important performance-limiting factor in PM motors is the heating of the permanent magnets, primarily caused by eddy currents induced by magnetic-field pulsations in the air gap. In slotted designs, these pulsations are significantly affected by the geometry of the stator slots, particularly the width of the slot opening. In contrast, pulsations in slotless motors arise solely from the space harmonics of the stator winding. Regardless of the source, these magnetic-field pulsations induce eddy currents in the magnets, leading to heating and reduced efficiency.

If all other motor parameters are equal, the torque, torque ripples, and heating of magnets determine whether a slotted or slotless design is preferable. Despite the existence of comprehensive comparative novel studies of slotted and slotless motors [6, 7], the results presented in those works cannot be easily applied to the performance comparison of specific motors. Therefore, a particular design requires a more in-depth investigation of the relevant phenomena and parameters.

This paper is devoted to the preliminary comparative study of torque and magnet heating in a slotless motor being developed, having the same main dimensions as a commercially available slotted external rotor motor [8]. The operating requirements include the ability of the motor to operate for a short time (about 60 s) with a current density of 20 A/mm². A specific feature of the developed slotless motor is its rotating internal "stator" yoke. This design requires the stator winding to be implemented as a compound cylindrical structure (sleeve-shaped), separated from the yoke by an air gap – just as it is separated from the rotor. Although this adds complexity to the winding design, it significantly simplifies the construction of both the stator and rotor cores, which can be manufactured as single solid parts using conventional turning machining technology. At

*ORCID: https://orcid.org/0000-0003-1416-1174

Fig. 1

the same time, the absence of relative motion in the stator yoke eliminates rotational iron losses, contributing to improved efficiency and potentially reducing overall production costs. There is significant experience with the development of such motor designs at the Institute of Electrodynamics, NAN of Ukraine [9]. The windings of the sleeve-shaped design and rotor are shown in Fig. 1. It should be noted that the presented design has magnets mounted on the inner yoke, whereas the motor under development is being designed to have magnets placed on the outer yoke.

Thus, the **aim of this study is** to analyze the differences in torque and permanent magnet heating under intensive operating conditions by comparing two specific alternative motor designs: slotted and slotless.

Designs and simulation software. Cross-sections of the two investigated designs are shown in Fig. 2, with corresponding parts highlighted using matching colors. The superscript "+" denotes current flowing out of the plane, while "–" indicates current flowing into the plane. Both designs feature an external rotor diameter of 40 mm and a magnetic core stack length of 20 mm. Motors of this size are typically manufactured with 14 rotor poles [8].

The main dimensions of the compared designs – namely, the rotor diameter, active length (stack), and air gap – are assumed to be equal. It is important to note that, according to the classical theory of electrical machines, the air gap in a slotless machine is equal to the design air gap plus the height of the winding. The cross-sectional areas of the windings are also equal thus current line loading A is equal . The external rotor is surrounded by an air layer to simulate the external magnetic flux linkage.

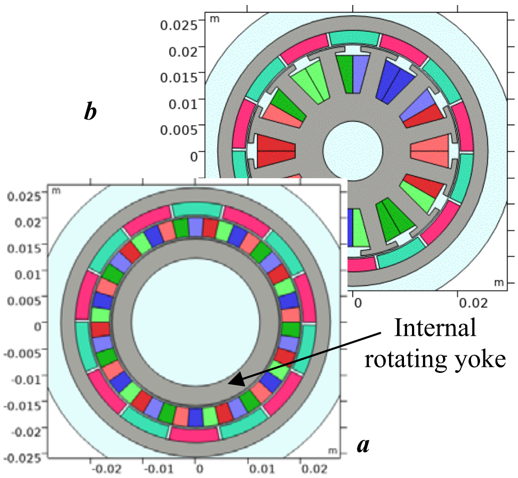

Fig. 2. Cross section of motors: a) slotless design; b) slotted design (red – A^+, dark red – A^-, green – B^+, dark green – B^-, blue – C^+, dark blue – C^-, purple – outward magnets, cyan – inward magnets, light cyan – air, gray - steel).

Common parameters	
Rotor speed	6000 rpm
Phase number	3
Rotor poles, p	14
Stator diameter, D (internal stator!)	40 mm
Stack length	20 mm
Air gap (between rotational parts)	0,5 mm
Height of rotor yoke	2,8 mm
Height of magnet, h_M	2,5 mm
Angular size of magnet	12°
Magnet type	N33SH
Remanent flux density, B_r	1,1 T
Winding fill factor	0,5
Recoil magnetic permeability, μ_{rec}	1,05
Max. effective current density J (≈ 60 s)	20 A/mm^2
Slotted design parameters	
Slot number	12
Slot height	8 mm
Tooth width	3,8 mm
Tooth crown head	1 mm
Slot opening width	3 mm
Slot wedge height	0,5 mm
Slotless design parameters	
Pole number	14
Internal air gap	0,5 mm
Height of winding, h_W	3,6 mm

The COMSOL Multiphysics software package was used for magnetic field simulation. To make the simulation domain more compact while preserving accuracy, a layer of infinite elements was placed at the outer boundary of the surrounding air region, which is not shown in Fig. 2. All necessary dimensions and parameters, both common and specific to the studied motors, are shown in Table. Consequently, the current density in the homogenized windings was equal in both designs.

As the study is comparative and not a comprehensive analysis, the following simulation settings and constraints were adopted according to the characteristics of the considered designs:

1. In the slotted design, the number of rotor poles and stator teeth is unequal. Thus, no symmetry can be identified in the cross section, and the magnetic field must be simulated over the entire cross-sectional domain. In con-

trast, the slotless design is characterized by equal stator and rotor pole pitches, which allows simulating the magnetic field over just two pole pitches.

2. Due to the consideration of eddy currents in the conductive parts of the machine (such as permanent magnets and yokes) and the presence of moving domains, time-dependent magnetic field modeling is required.
3. The magnetization characteristic was assumed to be nonlinear, and the yoke height and stator tooth width were chosen to ensure a magnetic flux density of approximately 1.7 T, as ensured by preliminary static magnetic field computations.
4. The current in the winding was assumed to be sinusoidal. This assumption is not critical for torque comparison. It is also not critical for magnet heating, as will be explained in the section devoted to heat analysis.
5. The rotational speed of the rotor was assumed to be constant.
6. The reference temperature T_0 of the magnets and windings before the intensive regime is 100 °C.

For the presented settings, the "Rotating Machinery" interface with a time-dependent study was used in the COMSOL Multiphysics software package. The investigation of permanent magnet heating was carried out using the "Heat Transfer in Solids and Fluids" interface of the same package [10]. This interface was essential to account for the convective cooling of the rotor's external surface by the surrounding air.

Torque analysis. The electromagnetic torque in COMSOL Multiphysics can be evaluated using two main approaches. The first is the Arkkio integration method, and the second is based on the Maxwell stress tensor [10]. For the slotless design, torque can also be calculated by integrating the Lorentz force over the winding domain. As expected, all methods yield similar results. Nevertheless, it should be noted that the Arkkio method demonstrates the highest stability, as indicated by the near equality of the positive and negative peaks in the evaluated torque. Integration of the Lorentz force provides comparable stability, but it is applicable only to the slotless design [10].

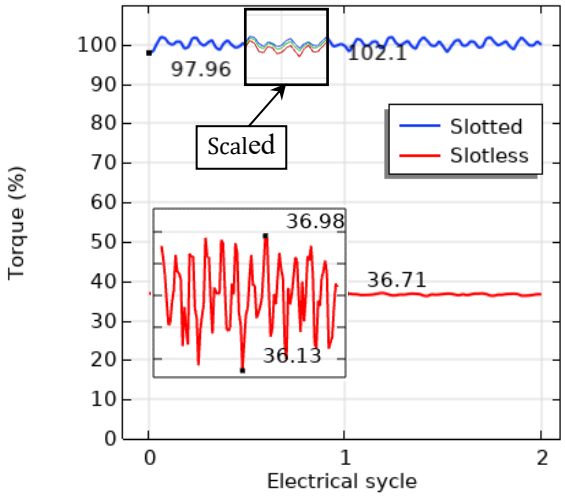

Fig. 3

To represent the torque difference between the studied designs, it is convenient to use relative units, taking the average torque of the slotted design as the reference value. The torque simulated over two electrical periods at effective current densities of 10, 15, and 20 A/mm² is shown in Fig. 3, where in each case the average torque of the slotted motor is taken as 100%. Due to the use of relative units, the curves corresponding to each design overlap. To illustrate this, a scaled fragment is shown in which the curves are artificially separated. From Fig. 3 it can be seen that the torque of the slotted motor is 2,7 times greater than that of the developed slotless motor. Moreover, torque pulsation in the slotted motor is 7,1 times higher than in the slotless one.

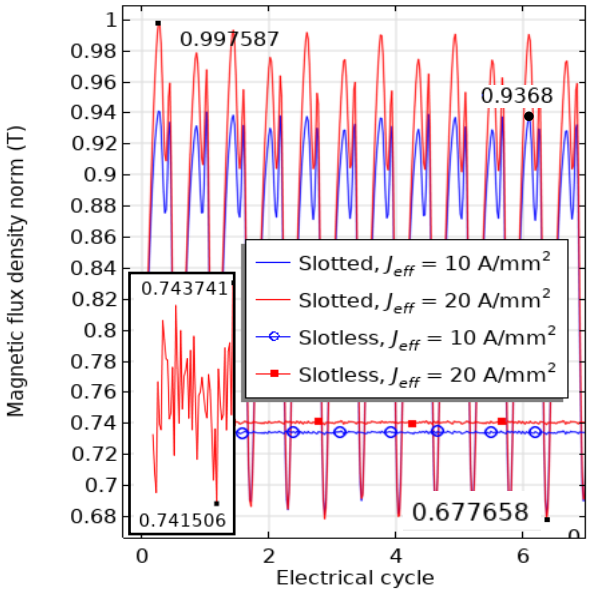

Fig. 4

The impact of this difference cannot be fully evaluated based solely on the ratio of magnetic flux densities along the midline of the air gap under steady-state conditions. As shown in Fig. 4, the ratio of the maximum flux densities is about 1,9, which is significantly lower than the torque ratio. It should be noted that in the slotless design, the magnetic flux density is evaluated at the center of the winding layer, which is valid only for torque computation using the Lorentz force integration method. The considerable torque reduction is mainly caused by the complex flux density distribution resulting

from the geometry of the stator tooth tips. Therefore, only integration using one of the aforementioned methods can provide an accurate estimate of the motor torque.

Evaluation of Permanent Magnet Heating. The heating of magnets is a harmful phenomenon in high-performance electric motors. The operating temperature limits of neodymium–iron–boron (NdFeB) magnets require precise evaluation of the heating process. Magnet heating is caused both by heat transfer through the air gap from the stator and by losses within the magnets themselves. As mentioned earlier, these losses result from eddy currents induced by magnetic field pulsations.

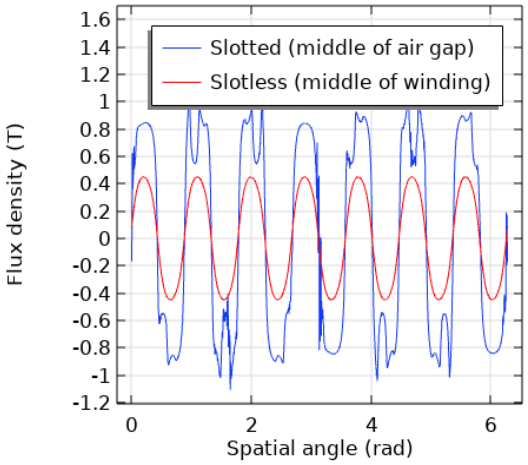

Fig. 5

Fig. 5 presents the distribution of the magnetic flux density norm over seven electrical cycles at an arbitrary point inside the magnet, situated near the surface facing the air gap and rotating with the magnet. The number of electrical cycles was chosen to cover a full cycle of the stator field in the machine. The magnetic flux density pulsation was evaluated at 10 and 20 A/mm² current densities in the winding.

In the slotted machine, this pulsation is caused mainly by the slotted structure of the stator magnetic core. The swing ΔB of the magnetic flux density B at the winding current density J =10 and 20 A/mm^2 is respectively

$$\Delta B_{J=10} = 0,9368 - 0,6777 = 0,2591(\text{T}); \quad \Delta B_{J=20} = 0,9976 - 0,6777 = 0,3199\ (\text{T}). \tag{1}$$

As the eddy current losses are proportional to the square of the magnetic flux density swing, it is natural to estimate the heating and temperature rise ratio of about

$$T / T_0 = \left(0,3199 / 0,2591\right)^2 = 1,52\,. \tag{2}$$

The slotless machine has the same number of poles in both the stator winding and the rotor structure. Thus, magnetic field pulsations are caused solely by the harmonic components of the stator winding magnetomotive force (MMF). However, in the magnified fragment of Fig. 5, high-frequency pulsations can also be observed. These are attributed to discretization errors and decrease with mesh refinement. To eliminate their influence on loss evaluation in "COMSOL Multiphysics", the *Time to Frequency Losses* subnode within the *Study* node was used. Losses in this subnode are evaluated through Fourier series decomposition, with the user specifying the number of harmonics. In this study, six time harmonics were taken into account to evaluate the eddy current losses, which provides the basis for further quantitative analysis. The Non-Ventilated cooling method was adopted to study. Note that the external rotor design is favorable for cooling.

A relevant question arises: should hysteresis losses be taken into account? The answer can be obtained by analyzing the range of magnetic flux density pulsations together with the demagnetization curve of the permanent magnet (PM). The demagnetization curve for the N33SH magnet is shown in Fig. 6 [11]. Owing to the extended linear portion of this curve, the entire flux density swing lies within the linear region. Therefore, hysteresis losses in the PM can be neglected.

After these preliminary remarks, the results of the investigated heating process can now be considered. As in the magnetic field simulation, the heat transfer computation was limited to a two-dimensional problem. The temperature distribution was simulated using the *Heat Transfer in Solids and Fluids* and *Turbulent Flow, Algebraic yPlus* interfaces of the "COMSOL Multiphysics" software package. Fig. 7 shows the temperature distribution in the rotor cross-section after one minute from the start of the intensive regime. The initial temperature T_0 was set to 100 °C, as mentioned above. In accordance with the previously analyzed magnetic flux pulsations (Fig. 5), the temperature rise in the slotted design is significantly more intensive than in the slotless one. Moreover, in the slotted design, heat is generated both in the solid rotor yoke and in the magnets themselves. The temperature scale in the legend of Fig. 7, *b* indicates that the hottest point in the slotted

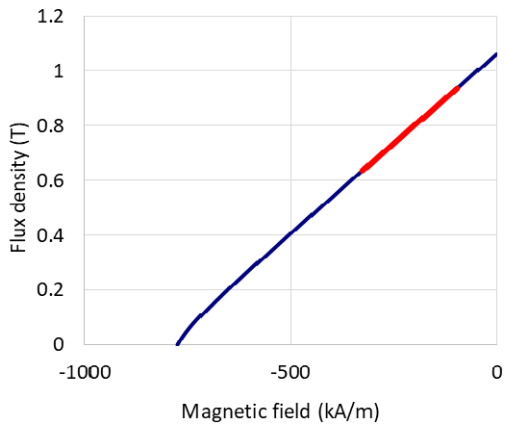

Fig. 6

design is heated by approximately 9,2 °C after one minute of operation at a current density of 20 A/mm². In contrast, in the slotless design, heat sources are concentrated primarily in the magnets, while the yoke does not contribute to magnet heating and acts as a heat sink (Fig. 7, *a*).

For verification, the maximum temperature rise in the magnets and winding of the slotted design was computed using the *Simcenter Motorsolve* software package. In this software, heat transfer is modeled with consideration of both radial and axial heat flow, but only approximately. The temperature rise of the magnets and winding of the slotted motor at three current density values (10, 15, and 20 A/mm²) is presented in Fig. 8. The maximum magnet temperature after 60 s, calculated with both software tools (Fig. 7, *b*, Fig. 8, *a*), is identical, thereby confirming the reliability of both models and the obtained results. The winding temperature rise in the slotted design reaches up to 135 °C (Fig. 8, *b*) under intensive operation, indicating that the winding insulation of classes F and H can withstand this regime.

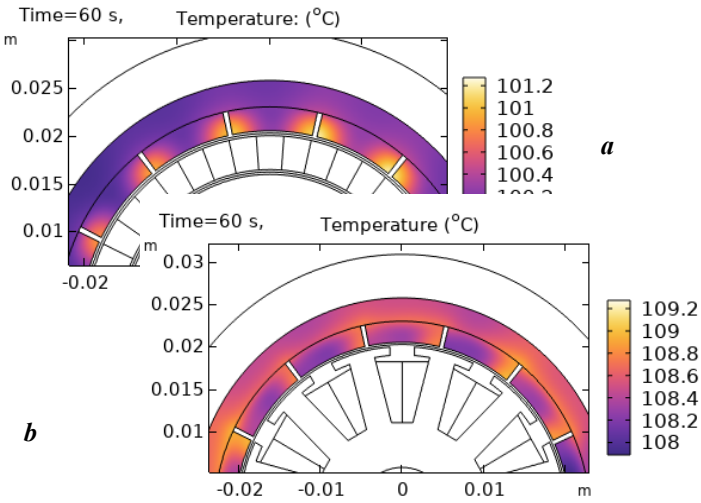

Fig. 7

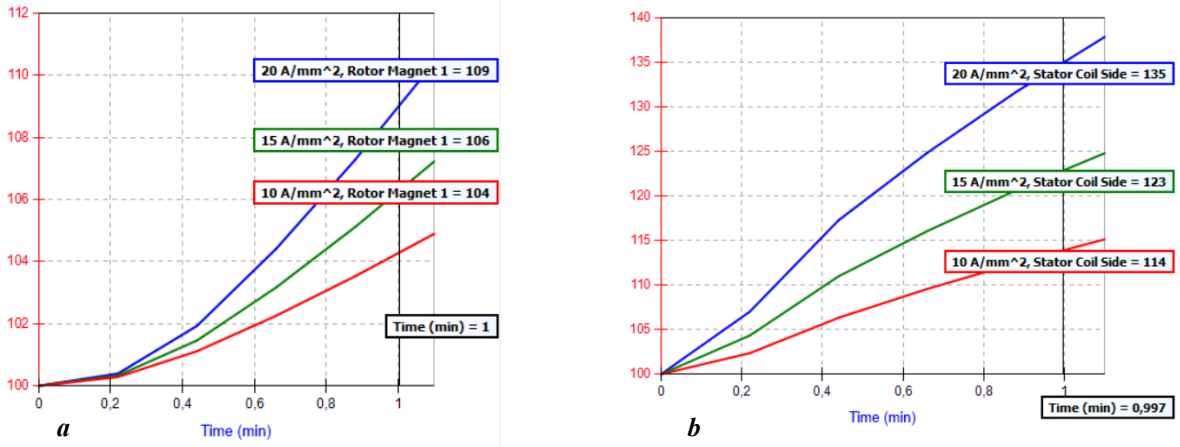

Fig. 8

In the slotless design, the temperature rise during 60 s is about 1.2 °C at J = 20 A/mm² (Fig. 7, *a*). Thus, there is no need to present temperature graphs at current densities below the maximum value. As for simulation in *Simcenter Motorsolve*, note that this software does not support designs with a rotated stator. Since the winding in this configuration is better cooled through two air gaps, it may be assumed that the winding temperature will remain within the same limits. The "COMSOL Multiphysics" software predicts a maximum winding temperature of about 40 °C after one minute of the intensive regime, which can be explained by the absence of axial heat transfer in the two-dimensional model.

Discussion. The slotted design exhibits the highest torque, which is approximately 2,7 times greater than that of the slotless one. The ratio of magnetic reluctances, considering only the non-steel segments of the magnetic circuit, is about 1,9, which corresponds to the ratio of the magnetic flux density amplitudes in the air gap (Fig. 4). The remaining factor of about 1,5 (the ratio between 2,7 and 1,9) can be attributed to the different geometric features of the windings.

The torque ratio of the two designs does not depend on the current density in the winding (Fig. 3). The reason is that the MMF of the winding F_W is significantly smaller than that of the magnet, so the mag-

netic flux is mainly determined by the magnet. More specifically, since the total current in both slotted and slotless designs is the same by assumption, the expression for the linear current loading A can be applied for either case. In fact, for the slotless design, within one pole pitch τ, this expression (taking into account the three-phase winding) is

$$A = \frac{3}{2}\frac{J(h_W \tau)}{\tau} = \frac{3}{2} 20 \cdot 10^6 \cdot 0,0036 = 108000 \left(\text{A/m}\right) , \quad (3)$$

where h_W is the winding height (geometrical and material parameters are given in Table 1). The half MMF of the winding F_W, providing the main magnetic flux, is

$$F_W = A \cdot \tau = A \frac{\pi D}{2p} = 108000 \frac{\pi \cdot 0,04}{2 \cdot 14} = 484,7 \left(\text{A}\right) , \quad (4)$$

where D is the stator diameter (noting that the design has an external rotor), p is the number of poles.

On the other hand the MMF of a single magnet F_M is

$$F_M = \frac{B_r h_M}{\mu_{rec} \mu_0} = \frac{1,1 \cdot 0,0025}{1,05 \cdot 4\pi \cdot 10^{-7}} = 2084 \left(\text{A}\right) , \quad (5)$$

where B_r is the remanent magnetic flux density, μ_{rec} is the recoil relative magnetic permeability, and h_M is the height of magnet. From expressions (4) and (5), it follows that the winding MMF is less than 25% of the magnet MMF.

The eddy current heating of the magnets is significantly higher in the slotted design. This is caused by the pronounced pulsation of the magnetic flux density. The swing of the flux density at an arbitrary point near the magnet surface reaches up to 0,32 T at a current density of 20 A/mm². The amplitude of this swing depends on the winding current density; at J = 10 A/mm², it is approximately 0,26 T. Since the ratio of these swings (see equation 2) provides an estimate of the magnet temperature rise rate of 1,52, the overheating of the slotted machine during one minute is given by (Fig. 8, *b*)

$$T_{20} / T_{10} = \left(109 - 100\right) / \left(104 - 100\right) = 2,25 . \quad (6)$$

The deviation of this value from 1,52 obtained in the single-harmonic analysis has a clear explanation: the time dependence of the magnetic flux density contains a significant share of higher harmonics (Fig. 5), which contribute additional losses. The remaining factor of about 1,48 (the ratio between 2,25 and 1,5).

Conclusions. Based on the investigations carried out, the torque and permanent magnet heating of a slotless, surface-mounted PM external-rotor motor can be estimated from the data of a series-produced slotted motor with identical geometric dimensions, within a certain range of comparable micromotor sizes.

The torque of the slotted design is approximately 2.7 times greater than that of the slotless machine and is independent of the current in the winding. This ratio can be derived from the ratio of the magnetic flux density amplitudes in the air gaps of the compared designs, using the coefficient defined in this paper.

The torque pulsation in the slotless design is about 7,1 times lower than that of the slotted motor.

In the slotted design, under the intensive regime with a winding current density of around 20 A/mm², the magnet temperature rises by approximately 9,2 °C per minute due to eddy currents. In the slotless design, under the same conditions, eddy current heating of the magnets due to magnetic field pulsations is much lower, resulting in a temperature rise of only about 1…2 %.

If either manufacturing cost or the minimisation of torque ripple is a primary concern, the slotless design may be preferred.

The work was supported by the state project "To develop scientific principles and principles of construction of magnetoelectric mechatronic modules for specialized automatic control systems" ("Mechatron"), KPKVK 6541030.

1. Islam M. S., Husain I., Mikail R. Slotless Lightweight Motor for Drone Applications. IEEE *Energy Conversion* Congress and Exposition (*ECCE*), Cincinnati, OH, 01-05 October 2017. DOI: https://doi.org/10.1109/ECCE.2017.8096851.

2. Lee Y.-S., Jang I.-S., Yang I.-J., Kim K.-S., Kim W.-H. Study on the Slotless PM Motor Design Process Considering High Speed. *IEEE Trans. Magn.* 2024. Vol 60. No 9. Pp. 1–4. DOI: https://doi.org/10.1109/TMAG.2024.3427729.

3. Chattopadhyay R., Islam M. S., Mikail R., Husain I. Slotless Motor with Active Metal Brazed Copper Winding for High Power Density Applications. 2022 IEEE *Energy Conversion* Congress and Exposition (*ECCE*), Detroit, MI, USA, 09-13 October 2022. Pp.1–7. DOI: https://doi.org/10.1109/ECCE50734.2022.9948146.
4. Petukhov I.S., Kireyev V.G., Akinin K.P., Lavrinenko V.A. Decreasing torque ripple of a slotless permanent magnet torque motor using a double-layer winding. *Tekhnichna Elektrodynamika*. 2024. No 4. Pp. 57–62. DOI: https://doi.org/10.15407/techned2024.04.057.
5. Celera Motion. Slotted vs Slotless Motors. URL: https://www.celeramotion.com/frameless-motors/support/technical-papers/slotless-vs-slotted-motors/ (accessed at 2025-06-14).
6. Nisarg Dave, Gaurang Vakil, Zeyuan Xu, Chris Gerada, He Zhang, David Gerada. Comparison of slotted and slotless PM machines for high kW/kg aerospace applications. 23rd International Conference on *Electrical Machines and Systems* (*ICEMS*), Hamamatsu, Japan, 24-27 November 2020. DOI: https://doi.org/10.23919/ICEMS50442.2020.9291221.
7. Min S.G., Sarlioglu B. Advantages and Characteristic Analysis of Slotless Rotary PM Machines in Comparison With Conventional Laminated Design Using Statistical Technique. *IEEE Trans. Transp. Electrification*. 2018. Vol 4. No 2. Pp. 517–524. DOI: https://doi.org/10.1109/TTE.2018.2810230.
8. Scorpion Power System. Scorpion SII-4020-630KV. URL: https://www.scorpionsystem.com/catalog/aeroplane/motors_1/sii-40/SII_4020-630/ (accessed at 2025-07-26).
9. Antonov A.E. Electric machines of magnetoelectric type. Fundamentals of Theory and Synthesis. Kyiv: Institute of Electrodynamics National Academy of Sciences of Ukraine, 2011. 216 p. (Rus)
10. COMSOL: Multiphysics Software for Optimizing Designs. COMSOL. URL: https://www.comsol.com/ (accessed at 2025-07-08).
11. Siemens. What's New in Simcenter Motorsolve and Simcenter SPEED 2021.1? URL: https://blogs.sw.siemens.com/simcenter/whats-new-in-simcenter-motorsolve-and-simcenter-speed-2021-1/ (accessed 2025-07-26).

УДК 621.313.84:531.383

КРУТНИЙ МОМЕНТ ТА НАГРІВАННЯ МАГНІТІВ У ДВИГУНІ З ПОВЕРХНЕВИМ РОЗТАШУВАННЯМ ПОСТІЙНИХ МАГНІТІВ: ПОРІВНЯННЯ ЗУБЧАСТОГО ТА БЕЗПАЗОВОГО СТАТОРА.

І.С. Пєтухов, Є.В. Ісаєв
Інститут електродинаміки НАН України,
пр. Берестейський, 56, Київ, 03057, Україна,
e-mail: igor_petu@ukr.net.

Проаналізовано переваги та недоліки двох конструкцій двигунів із постійними магнітами – із пазами та безпазової. Як зразок двигуна з пазами використано серійний мікродвигун. Їхню продуктивність порівняно за критеріями створення моменту і нагрівання постійних магнітів за умов інтенсивного режиму роботи. Геометрія ротора вважається однаковою, максимальна індукція в магнітопроводі обмежена рівнем 1,7 Тл, а швидкість обертання – сталою. Моделювання виконано в середовищі COMSOL Multiphysic. Задля перевірки результатів для двигуна з пазами використано програмний пакет Simcenter Motorsolve. Оцінено момент і амплітуду його пульсацій для обох конструкцій, проаналізовано відмінності між ними. Досліджено причини пульсацій магнітної індукції в магнітах і оцінено їхній вплив на вихрові втрати. Наведено числові результати співвідношень вихідних параметрів для двох конструкцій. Наголошено на можливості нехтування нагріванням магнітів у безпазовій конструкції. Бібл. 11, рис. 8, табл. 1.

***Keywords*:** двигун з постійними магнітами, крутний момент, втрати на вихрові струми, пазова конструкція, безпазова конструкція.

Received 28.07.2025
Accepted 09.10.2025